

# Strange Neutral Currents in Nuclei

M.T. Ressel

*W.K. Kellogg Radiation Laboratory, 106-38, California Institute of Technology, Pasadena, CA  
91125*

G.J. Mathews

*Department of Physics, University of Notre Dame, Notre Dame, IN 46556*

M.B. Aufderheide

*Department of Physics, University of Pennsylvania, Philadelphia, PA 19104  
and University of California, Lawrence Livermore National Laboratory, Livermore, CA 94550*

S.D. Bloom and D.A. Resler

*University of California, Lawrence Livermore National Laboratory, Livermore, CA 94550*

(February 9, 2008)

## Abstract

We examine the effects on the nuclear neutral current Gamow-Teller (GT) strength of a finite contribution from a polarized strange quark sea. We perform nuclear shell model calculations of the neutral current GT strength for a number of nuclei likely to be present during stellar core collapse. We compare the GT strength when a finite strange quark contribution is included to the strength without such a contribution. As an example, the process of neutral current nuclear de-excitation via  $\nu\bar{\nu}$  pair production is examined for the two cases.

**PACS: 13.15.+g, 21.60.Cs, 25.30.Pt, 97.60.Bw**

## I. INTRODUCTION

A number of recent experiments have provided tantalizing hints that the strange quark sea within the nucleon may play a major role in determining its physical properties. Most notably, the strange quarks may be polarized and a major contributor to the spin of the nucleon [1,2]. (The fraction of the proton's spin carried by the strange quark sea is usually denoted by  $\Delta s$ .) This interpretation is somewhat controversial [3], but remains the favored explanation of the experiments which measure the spin distribution of the nucleon. If the strange quark sea is polarized and contributes significantly to the nucleon's spin, then there are numerous implications for particle and nuclear physics as well as astrophysics. Among these are effects on neutral current interactions [4–8] and more exotic effects on processes such as neutralino-nucleus scattering (which is of fundamental importance in the search for particle dark matter [9]). In this paper, we focus upon inelastic neutrino-Nucleus,  $\nu A$ , interactions. In particular, we examine the effects of  $\Delta s \neq 0$  in the nucleon upon the neutral current Gamow-Teller (GT) strength in a number of nuclei that are present during supernova collapse.

The GT operator results from the axial-vector current in the non-relativistic and zero momentum-transfer limits (i.e. the allowed approximation). It is the dominant contribution in  $\nu A$  inelastic scattering. In the limit where strange quarks do not contribute to nucleonic properties (the standard case), the operator is purely isovector in nature. The inclusion of nucleonic spin due to polarized strange quarks, however, leads to an important change in the form of the GT operator. It acquires an *isoscalar* component! The zeroth order effect of this change is to increase the neutral current interaction strength of protons relative to that of neutrons [10]. This shift results in the redistribution of the neutral current GT strength function,  $B(GT_0)$ , for a nucleus. The inclusion of this isoscalar piece in the GT operator circumvents the usual isospin selection rule which forbids  $T = 0 \rightarrow T = 0$  transitions. This can open new transition channels and lead to a significant rearrangement of the low lying GT strength for  $T = 0$  nuclei. These new channels may present a method for a

precise measurement of  $\Delta s$  [7,8,11]. We briefly discuss this possibility in Section III. Also of importance is the effect of the redistribution of  $B(GT_0)$  upon the neutral current interaction rates. These rates are of interest as they may affect the neutrino distribution in core collapse supernovae.

It has been realized for some time that inelastic  $\nu A$  processes may play an important role in the pre- and post-collapse phases of supernovae [12–14]. The interaction rates for all of these inelastic processes are highly energy dependent and hence quite sensitive to the exact distribution of GT strength in nuclei. The neutral current GT strength distribution undergoes significant shifts if  $\Delta s$  differs appreciably from zero. Hence, the effects of strange quarks in the nucleon could have profound effects upon supernova dynamics. The effects of a non-zero value of  $\Delta s$  upon  $\nu$ -process nucleosynthesis [15] has previously been studied for several nuclei in the continuum random phase approximation [10]. Here we examine allowed neutral current GT processes which might play an important role in the heating and cooling of the collapsing star. As an example, we concentrate upon the process of nuclear de-excitation via the emission of a  $\nu\bar{\nu}$  pair (the neutral current analog of  $\beta$ -decay),  $A^* \longrightarrow A\nu\bar{\nu}$ . Because of phase space considerations, this process should be especially sensitive to  $\Delta s$  as well as being straightforward to calculate.

Supernova cores present an environment where nuclei may develop a large neutron excess. Since a finite  $\Delta s$  increases the strengths of  $\nu p$ , relative to  $\nu n$ , interactions there could conceivably be significant changes in the GT strength for nuclei with large neutron-proton asymmetry. An effect which will tend to compensate for this is Pauli blocking as the available neutron orbitals are filled. To investigate these two competing effects we examine the changes in  $B(GT_0)$  induced by a non-zero value of  $\Delta s$  in a series of iron isotopes with increasing  $N - Z$ . We will show that fairly significant changes in  $B(GT_0)$  can occur for very neutron rich nuclei.

Our calculations of  $B(GT_0)$  are performed in the nuclear shell model. This approach allows an accurate representation of the low lying strength, which is of paramount importance at the temperatures of interest.

## II. FORMALISM AND WAVE FUNCTIONS

The strange quark content of the nucleon plays a role in both the vector and axial-vector pieces of the weak hadronic current. The full formalism is presented in refs. [5,8,10]. Here we are concerned only with the axial-vector piece, which has the form

$$J_\mu^A = G_1(Q^2)\gamma_\mu\gamma_5, \quad (1)$$

where

$$G_1(Q^2) = -\frac{1}{2}G_A^3(Q^2)\tau_3 + \frac{1}{4}G_A^s(Q^2). \quad (2)$$

$G_A^3$  is the usual isovector coupling constant  $G_A^3(0) = g_A = 1.262$  and  $G_A^s$  is the isoscalar coupling arising because of the strange quarks in the nucleon. The EMC data implies a value of  $G_A^s(0) = -0.38 \pm 0.12$  [1,5,10] and we adopt this value here. Recent measurements by the SMC experiment [2] have found a slightly lower value for  $\Delta s$  and hence  $G_A^s$ . We use the larger, EMC value, to examine the maximum effect of the strangeness in the nucleon upon  $B(GT_0)$ . To make this even more pronounced, we quench the value of the isovector piece by the canonical amount, setting  $g_A = 1.0$ . The isospin operator has the values  $\tau_3 = +1(-1)$  for protons (neutrons).  $G_1(Q^2)$  is assumed to have the standard dipole form but this is irrelevant for this work since we work in the  $Q^2 \rightarrow 0$  limit.

In the zero momentum transfer and non-relativistic limits (valid for most supernova neutrinos) eqs. (1,2) lead to the neutral current GT operator

$$GT = -\frac{1}{2}(g_A\tau_3 - \frac{1}{2}G_A^s)\boldsymbol{\sigma}. \quad (3)$$

The familiar form is recovered if  $G_A^s = 0$ . It is immediately apparent that by including  $G_A^s \neq 0$  the GT operator will shift the relative strengths of the  $\nu p$  and  $\nu n$  interactions which are mediated by it. (e.g. taking  $g_A = 1$  and  $G_A^s = -0.38$ , we find  $GT|_{protons} = -0.595\boldsymbol{\sigma}$  and  $GT|_{neutrons} = 0.405\boldsymbol{\sigma}$ .) Also note, that since the operator is no longer purely isovector,  $T = 0 \rightarrow T = 0$  transitions are allowed and will be proportional to  $|G_A^s|^2$  [7,10]. Thus, we see that the presence of a non-zero  $G_A^s$  can lead to potentially important changes in the

matrix elements for  $\nu A$  interactions. To determine if this is indeed the case, the modified GT operator, eq. (3), needs to be evaluated between realistic nuclear wave functions and compared with the standard ( $G_A^s = 0$ ) results for various nuclei.

To examine the effect of the modified GT operator, eq. (3), upon  $\nu A$  reactions we have computed states for nuclei in the  $p$ ,  $sd$ , and  $fp$  shells. All of the wave functions and strength functions were generated using the nuclear shell model code CRUNCHER [16] and its auxiliary codes. We have studied the  $p$ -shell nuclei  $^{12}\text{C}$  and  $^{14}\text{N}$  using the Cohen-Kurath interaction [17]. The  $sd$ -shell nuclei  $^{20}\text{Ne}$ ,  $^{24}\text{Mg}$ , and  $^{28}\text{Si}$  were all investigated using the W, or universal  $sd$ , interaction [18]. In these two shells full basis  $0\hbar\omega$  calculations were performed.

In the  $fp$  shell, we performed calculations for  $^{56}\text{Ni}$  as well as a large series of iron isotopes using the fpvh interaction [19]. This interaction has been shown to reproduce excited state energy spectra [19] and charged current GT strength functions [20] with reasonable accuracy. We looked at the even-even isotopes of iron ranging from  $^{50}\text{Fe}$  to  $^{66}\text{Fe}$  to study the effect of increasing  $N - Z$  upon  $B(GT_0)$ . Because of the large dimensions of the  $fp$ -shell wave functions, we employed truncated model spaces for all of these nuclei. (A full basis calculation of  $^{56}\text{Fe}$  would have a m-scheme dimension of  $\sim 5 \times 10^8$ , far larger than can be accommodated using conventional diagonalization techniques.) In Table I, we present the list of  $fp$  shell nuclei examined in this work. We also list the model spaces considered and the m-scheme basis dimension for both the parent and daughter nuclei. Our daughter spaces are expanded so that we would satisfy the standard charged current sum rule.

In figure 1, we present the calculated and experimental excited state energy spectrum for the 10 lowest lying states of  $^{56}\text{Fe}$ . (The calculated spectrum is for the model space with basis dimension 8738 in Table I.) Figure 1 reveals quite good agreement between theory and experiment and supports the idea that the fpvh interaction in these model spaces produces good wave functions for these nuclei. Similarly good agreement is obtained for other nuclei with measured spectra.

Another piece of evidence which lends credence to these strength functions is the good

agreement between measured and calculated charged current GT strength functions. Aufderheide et al. [20] have found reasonable agreement between experiment and theory for several  $fp$ -shell nuclei using the fpvh interaction in similar model spaces. The agreement is much better for  $B(GT_-)$  than for  $B(GT_+)$  and, in any case, is not perfect since it requires the usual quenching factor in order to match the magnitude of the measured strength. On the whole, the distribution of strength is well reproduced in their calculations for sufficiently large model spaces. A similar level of accuracy is expected to hold for the neutral current processes calculated here.

### III. RESULTS

Kolbe, et al. [10] pointed out, that to first order, the ratio of the proton to neutron cross section varies as  $\sigma_p/\sigma_n \approx 1 + 2|G_A^s|/g_A$ . For  $G_A^s = -0.38$  and  $g_A = 1$  we find  $\sigma_p/\sigma_n = 1.76$  (for  $g_A = 1.262$ ,  $\sigma_p/\sigma_n = 1.60$ ). We see already that this effect may be important.

The total GT strength for a given nucleus is thought to scale roughly as [13]

$$B(GT_0) \propto \sum_{p,n} \sum_{i,f} |GT_{if}|^2 \frac{N_i^p N_f^h}{(2j_f + 1)} \quad (4)$$

where  $|GT_{if}| = \langle f|GT|i \rangle$  is a single particle transition matrix element between the states,  $N_i^p$  is the occupation number of the initial level,  $i$ , and  $N_f^h/(2j_f + 1)$  is the fractional number of holes in the final level,  $f$ . Eq. (4) is subject to the usual GT selection rules. Similar formulae have been used for charged current GT strength functions [21]. While detailed shell model studies have revealed inadequacies in such an approach for charged current interactions [20] as well as for the neutral currents [22], the above parameterization is quite useful for revealing general trends. For the modified operator of eq. (3) with  $G_A^s \neq 0$ , eq. (4) must be altered:

$$B(GT_0) \propto \sum_p \sum_{i,f} |GT_{if}(p)|^2 \frac{N_i^p(p) N_f^h(p)}{(2j_f(p) + 1)} + \sum_n \sum_{i,f} |GT_{if}(n)|^2 \frac{N_i^p(n) N_f^h(n)}{(2j_f(n) + 1)} \quad (5)$$

Here,  $p(n)$  denotes the proton (neutron) contribution to the strength. We see from eq. (5) that, since  $|GT_{if}(p)|^2 > |GT_{if}(n)|^2$ , the strength can be significantly altered for  $G_A^s \neq 0$ . However, for nuclei with  $N \approx Z$  the effects of the differing matrix elements will tend to cancel. For nuclei with  $|N - Z| \gg 0$ , fairly significant effects could be observed. Since many nuclei in the pre-collapse and collapse phases of a massive star's life cycle have  $N \gg Z$ , weak inelastic neutral current processes could undergo important changes.

A close examination of eq. (5) reveals several competing effects. As  $N - Z$  increases, the naive expectation is for  $B(GT_0)$  to decrease (relative to the  $G_A^s = 0$  case) because of the decrease in  $GT_{if}(n)$ . Looking at Table II, we see that this trend occurs for  $N - Z = -2$  to 4. For  $N - Z > 4$ , the strength, in iron, increases. This can be traced to the fact that the  $1f_{5/2}$  and  $2p_{1/2}$  neutron shells are starting to become occupied. This reduces the fractional number of holes available for the transition. This is the well known effect of Pauli shell blocking [23]. This shell blocking becomes increasingly important as the neutrons approach shell closure ( $N = 40$ ). For a completely closed neutron  $fp$  shell, Table II shows that inclusion of strange neutral currents leads to a 42 % increase in the total strength. In  $^{66}\text{Fe}$ , the strength is purely due to proton transitions. In figure 2 we plot  $\Delta B(GT_0)/B(GT_0)$  against  $N - Z$  for the series of iron isotopes considered. The competition between the altered matrix elements and shell blocking is clearly visible. We see that a significant change in  $B(GT_0)$  can occur in nuclei with a large neutron excess if strange quarks carry a reasonable fraction of the nucleon's spin.

In Table III we present the energy weighted centroid of the neutral current strength for the nuclei considered. No obvious correlation of the centroid with  $N - Z$  is apparent. Isotopes where the neutron transitions might be expected to dominate (large  $N_i^p(n)$  and  $N_f^h(n)/(2j_f(n) + 1)$ ) do seem to have slightly negative centroid shifts. Isotopes dominated by proton transitions (small  $N_i^p(n)$  or  $N_f^h(n)/(2j_f(n) + 1)$ ) tend to have a positive shift. In figure 3 we present the total strength function for  $^{58}\text{Fe}$  with and without a contribution due to strange quarks in the nucleon. This strength function is derived from transitions from 30 approximate eigenstates obtained by performing Lanczos iterations upon the Collective

Gamow-Teller state [24]. Transitions which are not converged are spread out over a Gaussian distribution with the appropriate width obtained from the computed second moments of the eigenstates. [22,24,25].

Although we have only considered the effects of increasing  $N - Z$  for a series of iron isotopes, there is nothing special about iron. We therefore expect similar behavior for most of the elements present during supernova core collapse. One set of elements where significant changes in  $B(GT_0)$  might occur are the  $T = 0$  ( $N = Z$ ) nuclei. These nuclei will not be abundant in the collapsing core but will be present in the outer envelopes of the star. As mentioned earlier, the presence of a non-zero  $G_A^s$  allows the GT operator to mediate  $T = 0 \rightarrow T = 0$  transitions. This has the effect of re-arranging the low lying GT strength. We now examine the magnitude of this effect.

In figures 4 and 5 we present the strength distributions for  $^{28}\text{Si}$  and  $^{56}\text{Ni}$ , both  $T = 0$  nuclei which will be abundant as a residue of thermonuclear burning in shells within and just above the collapsing core of a massive star. The solid line in each figure is the standard  $G_A^s = 0$  strength and the dotted line is the strength with  $G_A^s = -0.38$ . In each figure at least one new low lying isoscalar transition is apparent. There is also a shift in the shape of the resonance. This shift is primarily due to the change in convergence of the Lanczos vectors used to determine the strength distribution. For a more detailed discussion of the procedure used to obtain  $B(GT_0)$  see refs. [22,24,25].

Tables II and III show the quantitative shifts in the total strength and centroid of the  $T = 0$  nuclei respectively. There is a small, relatively constant, increase in the total strength of about 3 %. The one exception,  $^{14}\text{N}$ , has roughly a 6 % increase and is the only odd-odd nucleus considered here. We also see a fairly uniform slight decrease in the strength centroid for most of the nuclei considered. Thus, we see, that the redistribution of GT strength in  $T = 0$  nuclei is not likely to be a large effect.

To confirm the above statement, we must look at a real physical process. We choose the process  $A^* \rightarrow A\nu\overline{\nu}$ , neutral current de-excitation of a nucleus, in a hot stellar environment. This process is highly sensitive to the distribution of GT strength and hence should be



an excellent indicator of the possible importance of  $G_A^s \neq 0$  upon inelastic neutral current scattering processes in supernovae. This process has recently been considered in detail in ref. [22]. Here we sketch the details of the calculation.

We consider only decays to the ground state of the nucleus. Refs. [22,14] show that these decays dominate the rate for temperatures,  $T$ , less than about 1.5 MeV for  $fp$  shell nuclei. A more complete set of final states is required at higher  $T$ , but the effect we wish to emphasize is well illustrated by decay to this single state.

The neutrino pair energy emission rate from ground-state transitions of a thermal population of nuclear states is

$$\begin{aligned} \dot{\epsilon}_{\nu\bar{\nu}} = & 3.33 \times 10^{-4} \frac{g_a^2}{4} \sum_i |GT_{if}|^2 (E_i - E_f)^6 \\ & \times \frac{(2J_i + 1)e^{-E_i/T}}{G(Z, A, T)} \text{MeVsec}^{-1} \text{nucleus}^{-1}. \end{aligned} \quad (6)$$

Here,  $GT_{if}$  is now the matrix element connecting the shell model states ( $i$  = initial,  $f$  = final = ground state),  $E_i$  is the excited state energy,  $E_f = 0$  is the final state's energy,  $J_i$  is the initial state angular momentum, and  $G(Z, A, T)$  is the nuclear partition function. We see that there are two effects of a non-zero  $G_A^s$ . First, from the magnitude of the strength as represented by  $|GT_{if}|^2$ . Second, from the *location* of the strength through the factor  $(E_i - E_f)^6$ . This latter effect could be particularly important for  $T = 0$  nuclei where new states become available. In Table IV we present results for  $\dot{\epsilon}_{\nu\bar{\nu}}$ , for several of the calculated nuclei at  $T = 1$  MeV. In figures 6 and 7 we show  $\dot{\epsilon}_{\nu\bar{\nu}}$  as a function of temperature for  $^{56}\text{Ni}$  and  $^{28}\text{Si}$ . The turn over at  $T \sim 1.5$  MeV in  $^{56}\text{Ni}$  is an artifact of only considering ground state decay. It indicates the need to consider decay to more states than just the ground state above this temperature. Looking at Table IV and figures 6 and 7, it is once again evident that the effect of the strangeness content of the nucleon is typically of order a few percent for most nuclei.

$^{66}\text{Fe}$  is somewhat of an exception to the above statement. For this nucleus  $N = 40$  and there are *no* allowed neutron transitions in our model space. Thus, we see the full effect of the enhanced  $\nu p$  interaction strength. This is already obvious from the large value of

$\Delta B(GT_0)/B(GT_0)$  in Table II. This produces a commensurate increase in  $\dot{\epsilon}_{\nu\bar{\nu}}$ . Table IV shows that  $\dot{\epsilon}_{\nu\bar{\nu}}$  increases by  $\sim 40\%$  relative to the  $G_A^s = 0$  value at  $T \sim 1$  MeV. This is comparable to the naive estimates made at the beginning of section III. In figure 8 we show  $\dot{\epsilon}_{\nu\bar{\nu}}$  for the decay to the ground state as a function of temperature. Unfortunately, this large enhancement of neutrino energy emission is likely to occur only for nuclei with  $N = 40$ . If at any point in the collapse this condition is encountered, cooling due to neutral current de-excitation could be greatly enhanced. Additionally,  $fp$  shell nuclei with  $N = 40$  have no allowed electron capture strength, further increasing the significance of this process in this regime. Of course, excitations out of our model space into the  $sdg$  shell would tend to smooth over this enhancement by allowing the neutrons to once again contribute to the rate.

Other inelastic neutral current processes, such as both up and down  $\nu A$  scattering and  $\nu$  pair annihilation onto a nucleus ( $\nu\bar{\nu}A \rightarrow A^*$ ) will respond similarly to a non-zero  $G_A^s$ . For these processes, there will be identical shifts due to the altered matrix elements,  $GT_{if}$ , but the phase space will scale less steeply than the  $(E_i - E_f)^6$  factor encountered in eq. (6). Thus, we see that the strangeness content of the nucleon plays, at most, only a minor role in the energy exchange and transport in the collapsing cores of massive stars. (If the star passes through a regime where  $N = 40$  nuclei are extremely abundant, the strangeness might play a very important role.) The equally interesting question of the effect of  $G_A^s \neq 0$  upon  $\nu$ -process nucleosynthesis has been previously investigated in ref. [10].

We close this section by briefly mentioning the possibility of using inelastic neutral current  $\nu A$  scattering to determine  $G_A^s$ . This possibility has been explored for several nuclei in refs. [7,11]. One idea is to use a  $T = 0$  nucleus and look for a neutrino mediated transition to a  $T = 0$  excited state via its subsequent decay(s) to the ground state. In the regime where the allowed approximation applies, the  $\nu$  excitation cross section is proportional to  $|G_A^s|^2$ . Hence, an excitation to a  $T = 0$  state would determine a value for  $G_A^s$  (e.g. provided a sufficiently detailed and accurate nuclear model is available). The advantage of this method lies in the fact that the measurement is made in the  $Q^2 = 0$  limit where one would be

measuring  $\Delta s$  in the regime of interest. This stands in contrast to the accelerator experiments (e.g. EMC [1], SMC [2])) which measure  $\Delta s$  at large  $Q^2$ . The results then have to be extrapolated to the  $Q^2 = 0$  case. Since this extrapolation is through the non-perturbative regime, a great deal of uncertainty is introduced. While this method is extremely attractive from a theoretical standpoint, it is a challenging experimental task at best.

#### IV. CONCLUSIONS

In this paper we have examined the consequences of a non-negligible value of  $\Delta s$  (or equivalently,  $G_A^s$ ) upon inelastic  $\nu A$  interactions. We have focused upon neutral current Gamow-Teller processes for a number of nuclei that might be relevant for core collapse supernovae. All of the calculations have been done in the nuclear shell model in order to obtain an accurate representation of the Gamow-Teller strength,  $B(GT_0)$ . We have focused upon two aspects of the modified GT operator, eq. (3). The first of these is the deviation, from the  $G_A^s = 0$  case, as the value of  $N - Z$  changes. The second is the changes in  $B(GT_0)$  for  $T = 0$  nuclei which result from the isoscalar piece in eq. (3). Most of our discussion focuses upon the strength function,  $B(GT_0)$ , but we have also examined a real physical process which may be important in core collapse supernovae, i.e. the process  $A^* \rightarrow A\nu\bar{\nu}$ . This nuclear de-excitation should be especially sensitive to  $G_A^s$  due to its steep dependence upon the excitation energy.

In the initial collapse of a massive star's core, nuclei will become very neutron rich,  $N \gg Z$ . The inclusion of a non-zero  $G_A^s$  would then change the ratio of  $\nu p$  and  $\nu n$  interaction strengths leading to a redistribution in GT strength. This redistribution should become more pronounced as  $N - Z$  increases. In tables II and III we presented our results for both  $B(GT_0)$  and its centroid with  $G_A^s = 0$  and  $G_A^s = -0.38$  for a series of iron isotopes with  $-2 \leq N - Z \leq 14$ . We found that  $B(GT_0)$  initially decreased as  $N$  increased, in line with expectations. As the neutron  $1f_{5/2}$  and  $2p_{1/2}$  orbitals began to fill, shell blocking became important. At this point, proton transitions began to dominate the strength. Thus for large

$N - Z$  there was a steady increase in  $B(GT_0)$ . This change was typically of order 10 % but reached  $\sim 40\%$  for  $^{66}\text{Fe}$ . Since there were no new transitions added, just a reweighting of those already present, there was very little change in the position of the strength's centroid. This implies that the change in  $\dot{\epsilon}_{\nu\bar{\nu}}$ , eq. (6) is predominately controlled by the change in  $B(GT_0)$  and the large phase space factor does not come into play.

For  $T = 0$  nuclei, the story is somewhat different. For these nuclei  $G_A^s \neq 0$ , which leads to a violation of the standard no  $T = 0 \rightarrow T = 0$  selection rule for GT transitions. Thus, new interaction channels become available and a significant rearrangement of the strength becomes possible. We studied  $B(GT_0)$  in a number of  $T = 0$  nuclei and found only about a 3-6 % change in  $B(GT_0)$  and only a small shift for its centroid. The results are presented in Tables II and III. We find that despite new channels opening up, the total strength is only slightly modified. Nevertheless, these new channels do, perhaps, present an intriguing method for measuring  $\Delta s$  even though the strength present in these new channels is insufficient to cause a major change in the energy emission rate for the nuclear de-excitation process considered.

We close by noting that a non-zero  $G_A^s$  seems unlikely to produce a significant change in calculated neutral current GT processes [22,14]. The effects are not entirely negligible but will not severely change the dominant neutrino energy emission mechanisms. This is especially true in that we have used a value of  $|G_A^s|$  which is probably too large (the SMC finds a smaller, but non-zero, value [2]). Also, we have quenched  $g_A$  but not  $G_A^s$ . In that sense, the results presented here should be regarded as upper limits.

## ACKNOWLEDGMENTS

Work at LLNL was performed under the auspices of the U.S. Department of Energy under contract W-7405-ENG-48 M.A. acknowledges support from the U.S. Department of Energy under contract DOE-AC02-76-ERO-3071. M.T.R. acknowledges support from the Weingart foundation and the U.S. National Science Foundation under Grants PHY94-12818

and PHY94-20470. Work at the University of Notre Dame supported by DOE Nuclear Theory Grant DE-FG02-95ER-40934.

## REFERENCES

- [1] J. Ashman, et al., Nucl. Phys. **B 328**, 1 (1989).
- [2] B. Adeva, et al., Phys. Lett. **B 302**, 533 (1993); J. Ellis and M. Karliner, Phys. Lett. **B 313**, 131 (1993).
- [3] R.L. Jaffe and A. Manohar, Nucl. Phys. **B337**, 509 (1990).
- [4] D.B. Kaplan and A. Manohar, Nucl. Phys. **B310**, 527 (1988).
- [5] E.J. Beise and R.D. McKeown, Comments Nucl. Part. Phys. **20**, 105 (1991).
- [6] J. Bernabú, T.E.O. Ericson, E. Hernández, and J. Ros, Nucl. Phys. **B 378**, 131 (1992).
- [7] T. Suzuki, Y. Kohyama, and K. Yazaki, Phys. Lett. **B 252** 323 (1990).
- [8] G. Garvey, et al., Phys. Rev. **C 48**, 1919 (1993).
- [9] M.T. Ressell, et al., Phys. Rev. **D 48**, 5519 (1993); K. Griest, Phys. Rev. **D 38**, 2357 (1988); J. Ellis and R. Flores, Nucl. Phys. **B307**, 883 (1988).
- [10] E. Kolbe, K. Langanke, S. Krewald, and F.K. Thielemann, Astrophys. J. **410** L89 (1992).
- [11] E.M. Henley, et al., Phys. Lett. **B 269**, 31 (1991).
- [12] E.W. Kolb and T.J. Mazurek, Astrophys. J. **234**, 1085 (1979).
- [13] G.M. Fuller and B.S. Meyer, Astrophys. J. **376**, 701 (1991).
- [14] S.W. Bruenn and W.C. Haxton, Astrophys. J. **376**, 678 (1991).
- [15] S.E. Woosley, D.H. Hartmann, R.D. Hoffman, and W.C. Haxton, Astrophys. J. **356**, 272 (1990).
- [16] D.A. Resler and S.M. Grimes, Comput. in Phys. **2** (3), 65 (1988).
- [17] S. Cohen and D. Kurath, Nucl. Phys. **73**, 1 (1965).

- [18] B.H. Wildenthal, in *Progress in Particle and Nuclear Physics*, edited by D.H. Wilkinson (Pergamon, Oxford, England, 1984), Vol. 11, p.5.
- [19] A. van Hees and P. Glaudemans, Z. Phys. **A 303**, 267, (1981); J. van Heinen, W. Chung, and B.H. Wildenthal, Z. Phys. **A 269**, 159 (1976).
- [20] M.B. Aufderheide, et al., Phys. Rev. **C 48**, 1677 (1993).
- [21] G.M. Fuller, W.A. Fowler, and M.J. Newman, Astrophys. J. **252**, 715 (1982).
- [22] M.T. Ressell et al., in preparation (1994).
- [23] G.M. Fuller, Astrophys. J. **252**, 741 (1982).
- [24] G.J. Mathews, et al., Phys. Rev. **C 32**, 796 (1985).
- [25] S.D. Bloom and G.M. Fuller, Nucl Phys. **A440**, 511 (1985).
- [26] C.M. Lederer and V.S. Shirley, *Table of Isotopes*, 7th ed. (John-Wiley, New York, 1978).

## FIGURES

FIG. 1. The calculated (left) and measured [26] (right) excited state energy spectrum of  $^{56}\text{Fe}$ . The calculated spectrum was obtained using the fpvh interaction [19] in the daughter model space described in Table I. The ground state has  $J^\pi = 0^+$ . The  $J^\pi$  values of many of the low lying states have been included for reference.

FIG. 2. The change in the Gamow-Teller strength in a series of iron isotopes ( $Z = 26$ ) due to the strangeness in the nucleon as a function of  $N - Z$ .

FIG. 3. The total neutral current Gamow-Teller strength function for  $^{58}\text{Fe}$ . The solid line is the result using the standard ( $G_A^s = 0$ ) result. The dashed line shows the effects of including  $G_A^s = -0.38$  in the operator of eq. (3).

FIG. 4. The total neutral current Gamow-Teller strength function for  $^{28}\text{Si}$ . The solid line is the result using the standard ( $G_A^s = 0$ ) result. The dashed line shows the effects of including  $G_A^s = -0.38$  in the operator of eq. (3). Note the two  $T = 0 \rightarrow T = 0$  transitions at 7.94 MeV and 9.40 MeV which are not present in the standard result. Also note that the change in appearance in the  $T = 1$  peak at 10.81 MeV is primarily due to the altered convergence properties of the Lanczos iterations used to obtain the strength distribution.

FIG. 5. The total neutral current Gamow-Teller strength function for  $^{56}\text{Ni}$ . The solid line is the result using the standard ( $G_A^s = 0$ ) result. The dashed line shows the effects of including  $G_A^s = -0.38$  in the operator of eq. (3). Note the  $T = 0 \rightarrow T = 0$  transition at 6.43 MeV. Also note that the change in appearance of the  $T = 1$  peaks near 10 MeV is primarily due to the altered convergence properties of the Lanczos iterations used to obtain the strength distribution.

FIG. 6. The neutrino energy emission rate for the process  $A^* \rightarrow A\nu\bar{\nu}$  ( $\dot{\epsilon}_{\nu\bar{\nu}}$ , eq. (6)) as a function of Temperature for  $^{28}\text{Si}$ . The rate includes only decay to the ground state.

FIG. 7. The neutrino energy emission rate for the process  $A^* \rightarrow A\nu\bar{\nu}$  ( $\dot{\epsilon}_{\nu\bar{\nu}}$ , eq. (6)) as a function of Temperature for  $^{56}\text{Ni}$ . The rate includes only decay to the ground state.



FIG. 8. The neutrino energy emission rate for the process  $A^* \rightarrow A\nu\bar{\nu}$  ( $\dot{\epsilon}_{\nu\bar{\nu}}$ , eq. (6)) as a function of Temperature for  $^{66}\text{Fe}$ . The rate includes only decay to the ground state. The large enhancement over the  $G_A^s = 0$  case can be traced to the fact that this nucleus has no allowed neutron transitions in this model space.

# TABLES

TABLE I. The model spaces used for calculating  $B(GT_0)$  for  $fp$  shell nuclei. Columns 2 and 3 list the parent model space and m-scheme dimension. Columns 4 and 5 list the same for the daughter nucleus' space.

Nucleus	Parent Model Space	Dim.	Daughter Model Space	Dim.
$^{50}\text{Fe}$	$(1f_{7/2})^{10,9}(2p_{3/2}2p_{1/2}1f_{5/2})^{0,1}$	5350	$(1f_{7/2})^{10,9,8}(2p_{3/2}2p_{1/2}1f_{5/2})^{0,1,2}$	67948
$^{52}\text{Fe}$	$(1f_{7/2})^{12,11}(2p_{3/2}2p_{1/2}1f_{5/2})^{0,1}$	3160	$(1f_{7/2})^{12,11,10}(2p_{3/2}2p_{1/2}1f_{5/2})^{0,1,2}$	57710
$^{54}\text{Fe}$	$(1f_{7/2})^{14,13}(2p_{3/2}2p_{1/2}1f_{5/2})^{0,1}$	328	$(1f_{7/2})^{14,13,12}(2p_{3/2}2p_{1/2}1f_{5/2})^{0,1,2}$	10620
$^{56}\text{Fe}$	$(1f_{7/2})^{14}(2p_{3/2}2p_{1/2}1f_{5/2})^2$	200	$(1f_{7/2})^{14,13}(2p_{3/2}2p_{1/2}1f_{5/2})^{2,3}$	8738
$^{58}\text{Fe}$	$(1f_{7/2})^{14}(2p_{3/2}2p_{1/2}1f_{5/2})^4$	1392	$(1f_{7/2})^{14,13}(2p_{3/2}2p_{1/2}1f_{5/2})^{4,5}$	46310
$^{60}\text{Fe}$	$(1f_{7/2})^{14}(2p_{3/2}2p_{1/2}1f_{5/2})^6$	2542	$(1f_{7/2})^{14,13}(2p_{3/2}2p_{1/2}1f_{5/2})^{6,7}$	72298
$^{62}\text{Fe}$	$(1f_{7/2})^{14}(2p_{3/2}2p_{1/2}1f_{5/2})^8$	1392	$(1f_{7/2})^{14,13}(2p_{3/2}2p_{1/2}1f_{5/2})^{8,9}$	35482
$^{64}\text{Fe}$	$(1f_{7/2})^{14,13}(2p_{3/2}2p_{1/2}1f_{5/2})^{10,11}$	4638	$(1f_{7/2})^{14,13,12}(2p_{3/2}2p_{1/2}1f_{5/2})^{10,11,12}$	37360
$^{66}\text{Fe}$	$(1f_{7/2})^{14,13,12,11}(2p_{3/2}2p_{1/2}1f_{5/2})^{12,13,14,15}$	1710	$(1f_{7/2})^{14,13,12,11,10}(2p_{3/2}2p_{1/2}1f_{5/2})^{12,13,14,15,16}$	3102
$^{56}\text{Ni}$	$(1f_{7/2})^{16,15,14}(2p_{3/2}2p_{1/2}1f_{5/2})^{0,1,2}$	1353	$(1f_{7/2})^{16,15,14,13}(2p_{3/2}2p_{1/2}1f_{5/2})^{0,1,2,3}$	34593

TABLE II. The change in the total neutral current GT strength,  $B(GT_0)$ . Column 3 lists  $B(GT_0)$  with  $G_A^s = 0$ , column 4 lists  $B(GT_0)$  with  $G_A^s = -0.38$ , and column 5 lists the change between the two divided by the  $G_A^s = 0$  value.

Nucleus	$N - Z$	$B(GT_0) _{G_A^s=0}$	$B(GT_0) _{G_A^s=-0.38}$	$\Delta B(GT_0) / B(GT_0) _{G_A^s=0}$
$^{50}\text{Fe}$	-2	17.3521	19.2245	0.108
$^{52}\text{Fe}$	0	20.3881	21.1276	0.036
$^{54}\text{Fe}$	2	24.0775	23.6927	-0.016
$^{56}\text{Fe}$	4	23.7421	23.5076	-0.01
$^{58}\text{Fe}$	6	21.4906	22.0658	0.027
$^{60}\text{Fe}$	8	19.6358	20.8826	0.064
$^{62}\text{Fe}$	10	17.1889	19.2029	0.117
$^{64}\text{Fe}$	12	14.3119	17.2748	0.207
$^{66}\text{Fe}$	14	8.4445	11.9583	0.416
$^{56}\text{Ni}$	0	23.9834	24.7462	0.032
$^{28}\text{Si}$	0	7.7844	8.0314	0.032
$^{24}\text{Mg}$	0	4.6568	4.8198	0.035
$^{20}\text{Ne}$	0	10.9113	11.3027	0.036
$^{14}\text{N}$	0	4.6276	4.8938	0.058
$^{12}\text{C}$	0	2.0906	2.1555	0.031

TABLE III. The change in the location (in MeV) of the energy weighted centroid of the GT strength for all of the nuclei studied. Column 3 lists the centroid with  $G_A^s = 0$ , column 4 lists the centroid with  $G_A^s = -0.38$ , and column 5 lists the change in the position.

Nucleus	$N - Z$	Centroid( $G_A^s = 0$ )	Centroid( $G_A^s = -0.38$ )	$\Delta$ Centroid
$^{50}\text{Fe}$	-2	12.4738	12.5194	0.041
$^{52}\text{Fe}$	0	13.0520	12.9440	-0.108
$^{54}\text{Fe}$	2	13.2015	13.0450	-0.157
$^{56}\text{Fe}$	4	11.473	11.336	-0.137
$^{58}\text{Fe}$	6	11.7908	11.7161	-0.075
$^{60}\text{Fe}$	8	11.7007	11.7458	0.045
$^{62}\text{Fe}$	10	11.2949	11.4172	0.122
$^{64}\text{Fe}$	12	11.6246	11.6335	0.009
$^{66}\text{Fe}$	14	11.1195	11.1195	0.0
$^{56}\text{Ni}$	0	10.3315	10.2217	-0.110
$^{28}\text{Si}$	0	13.5540	13.4686	-0.075
$^{24}\text{Mg}$	0	13.4006	13.3583	-0.042
$^{20}\text{Ne}$	0	15.8091	15.8346	0.026
$^{14}\text{N}$	0	9.8878	9.6560	-0.232
$^{12}\text{C}$	0	15.6493	15.5642	-0.085

TABLE IV. The value of the energy emission rate for the process  $A^* \rightarrow A\nu\bar{\nu}$ ,  $\epsilon_{\nu\bar{\nu}}$  in eq. 6, in MeV/sec/Nucleus for several nuclei.

Nucleus	$G_A^s = 0$	$G_A^s = -0.38$	Change
$^{56}\text{Fe}$	0.03944	0.04168	5.7 %
$^{58}\text{Fe}$	0.02228	0.02362	6.0 %
$^{62}\text{Fe}$	0.01093	0.01209	10.1 %
$^{64}\text{Fe}$	0.00627	0.00744	18.6 %
$^{66}\text{Fe}$	0.00385	0.00546	41.6 %
$^{56}\text{Ni}$	0.25095	0.26501	5.6 %
$^{28}\text{Si}$	0.04577	0.04882	6.7 %

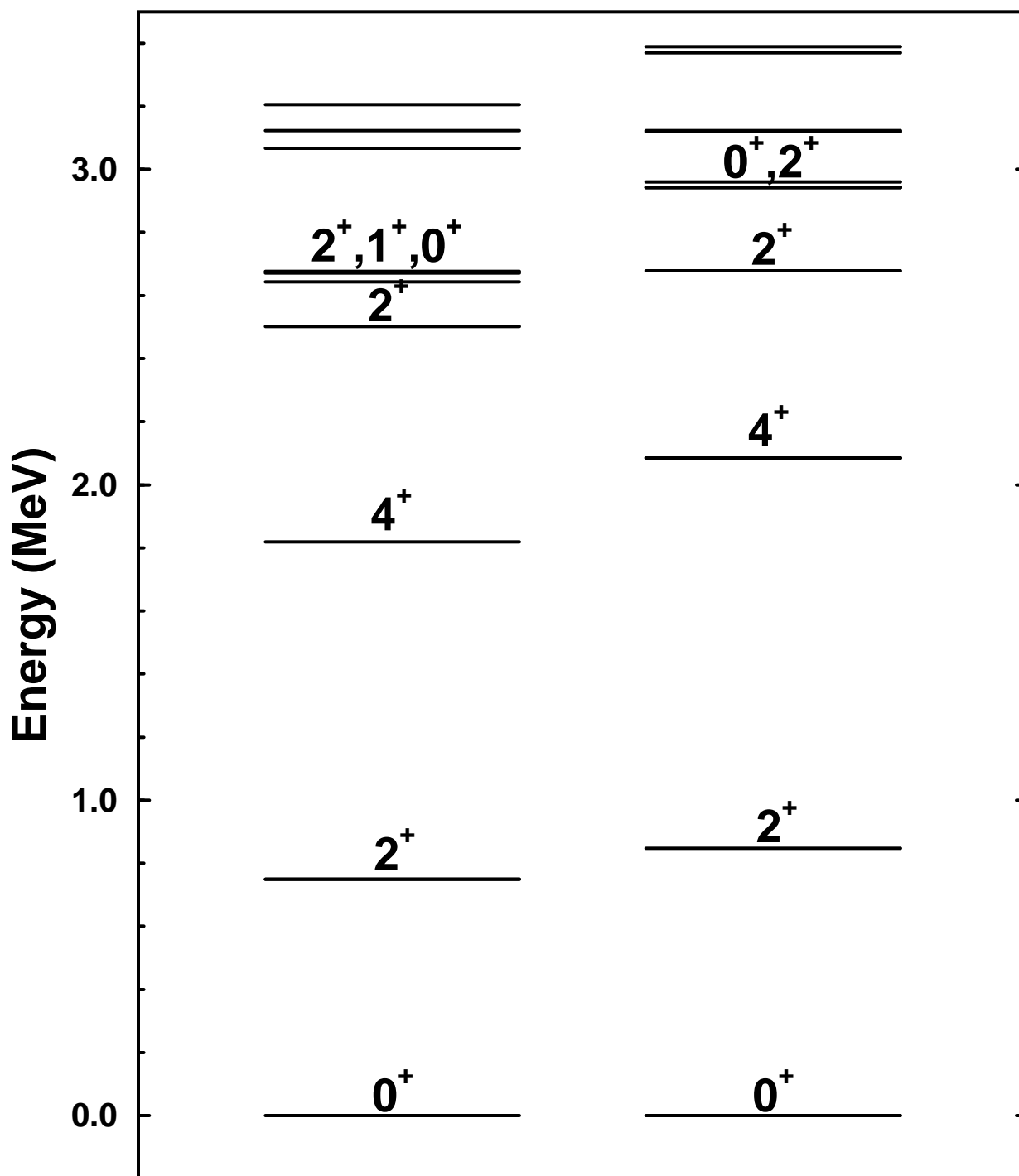


Figure 1

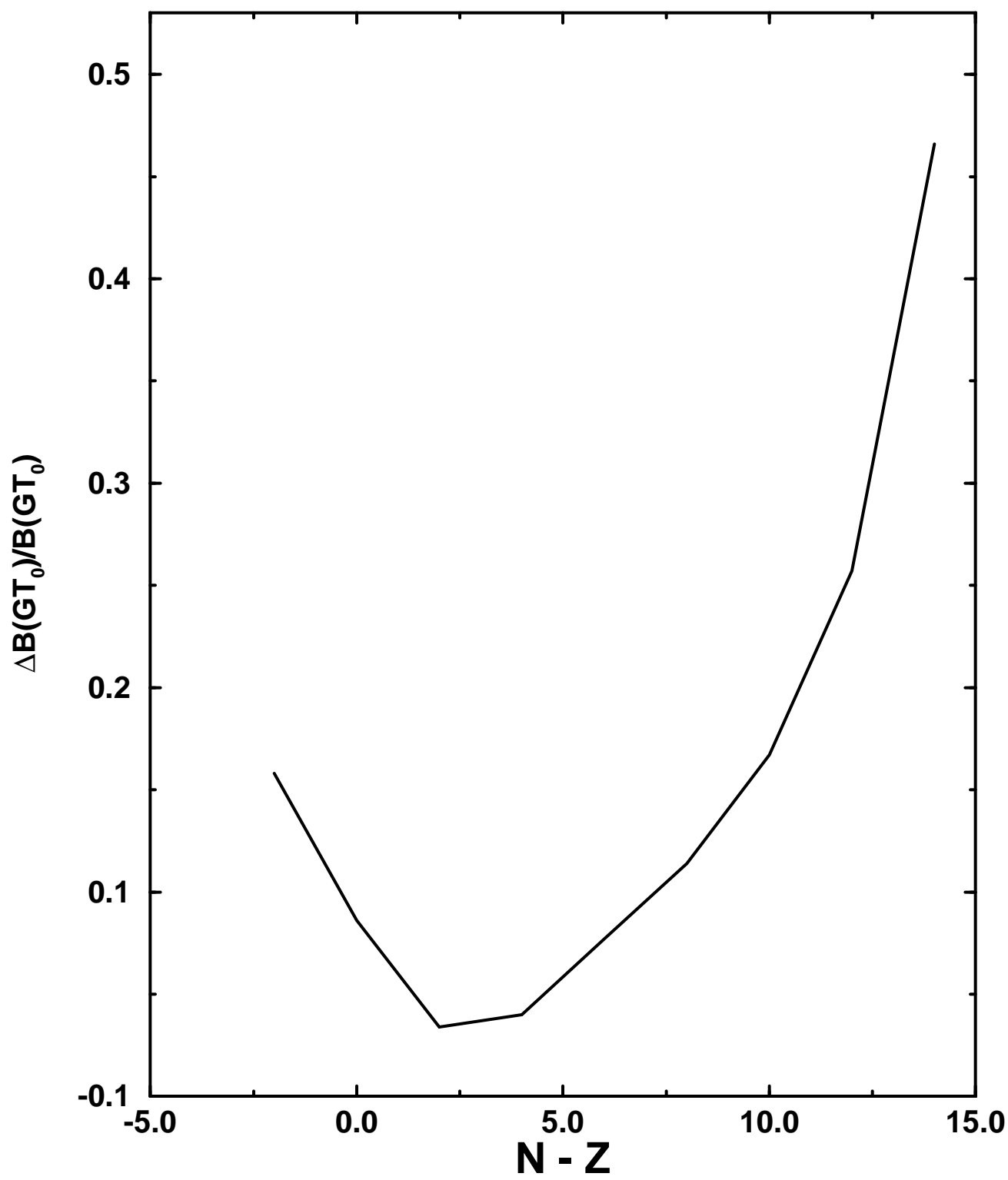


Figure 2

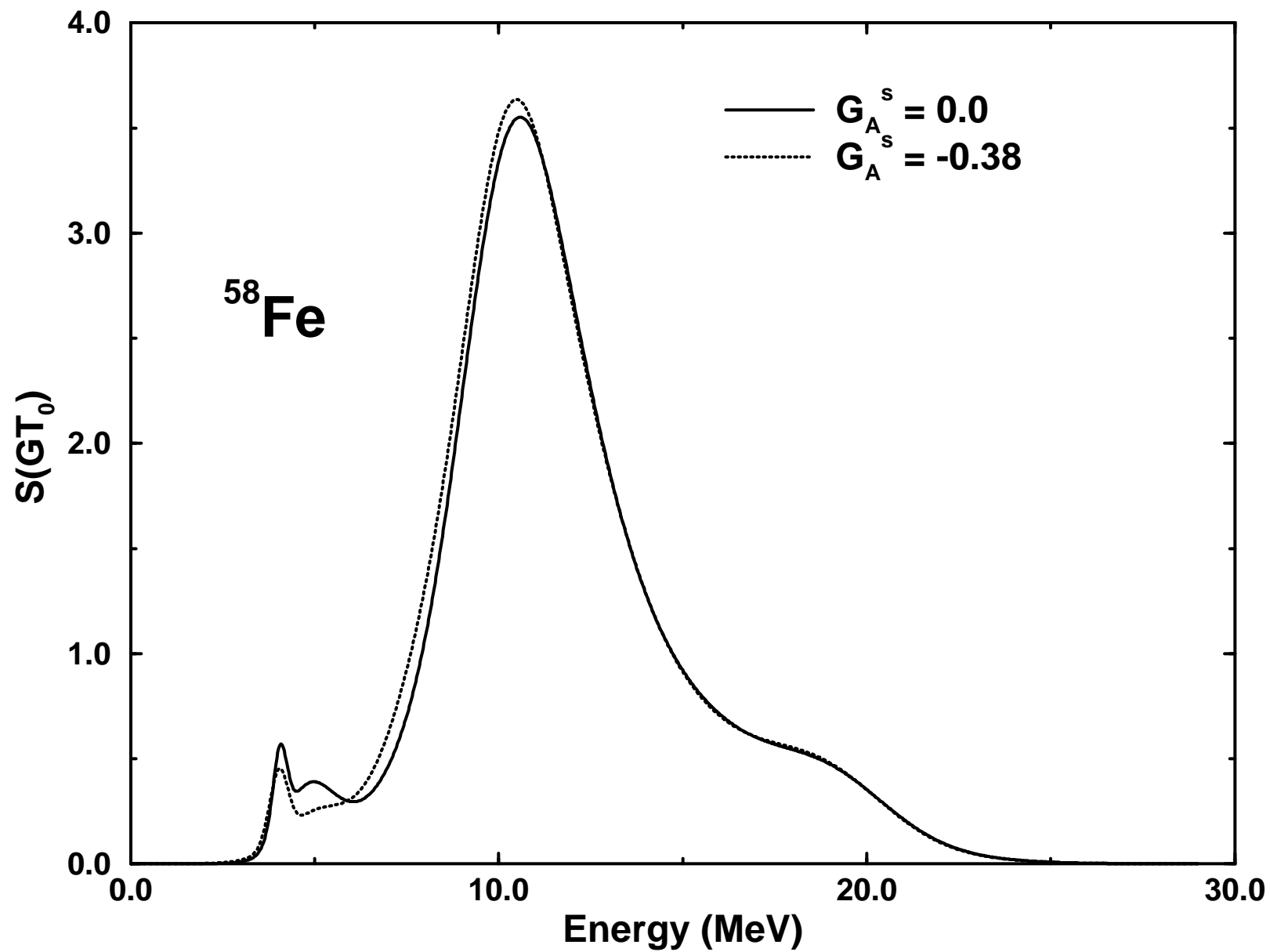


Figure 3

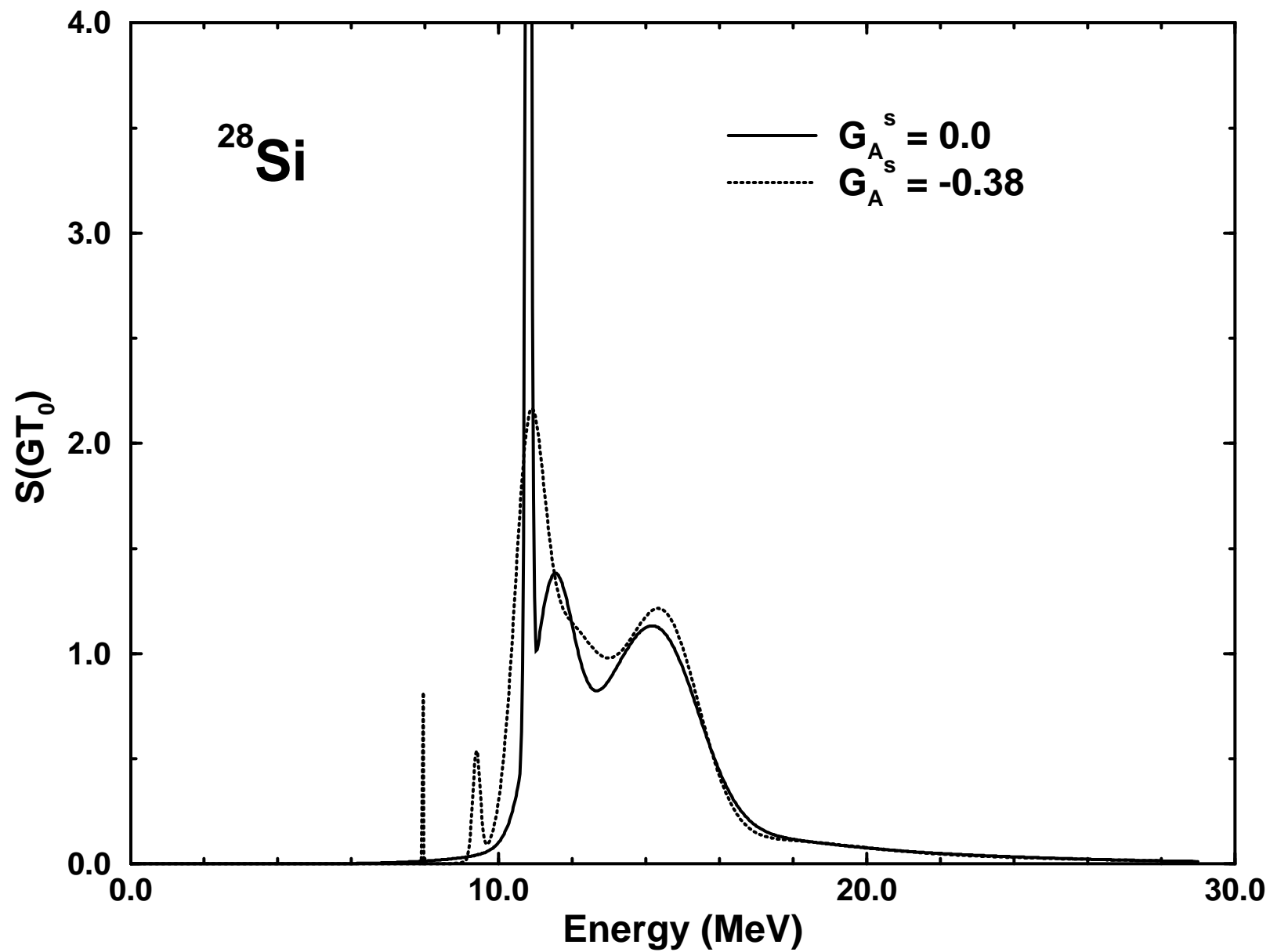


Figure 4



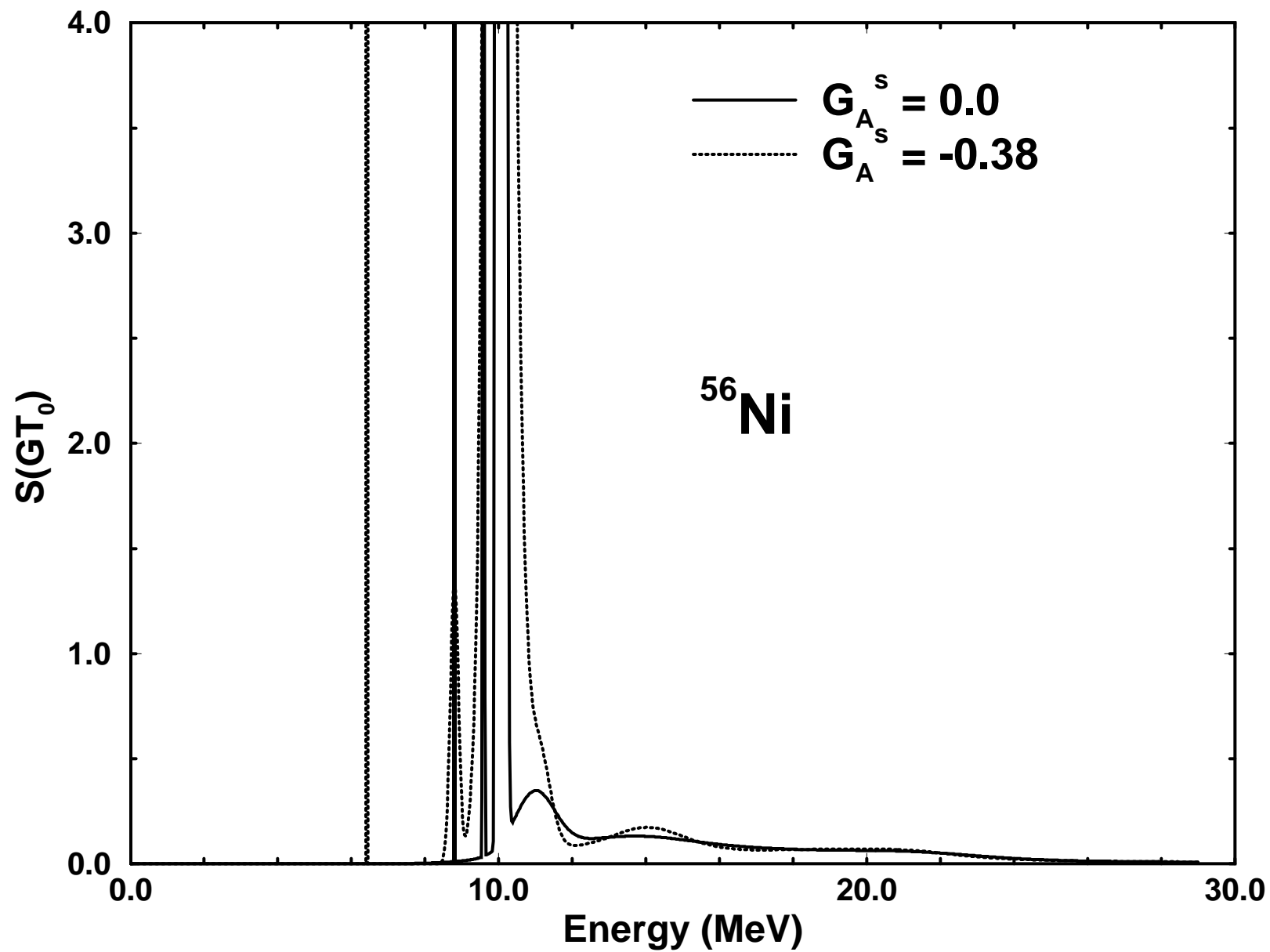


Figure 5

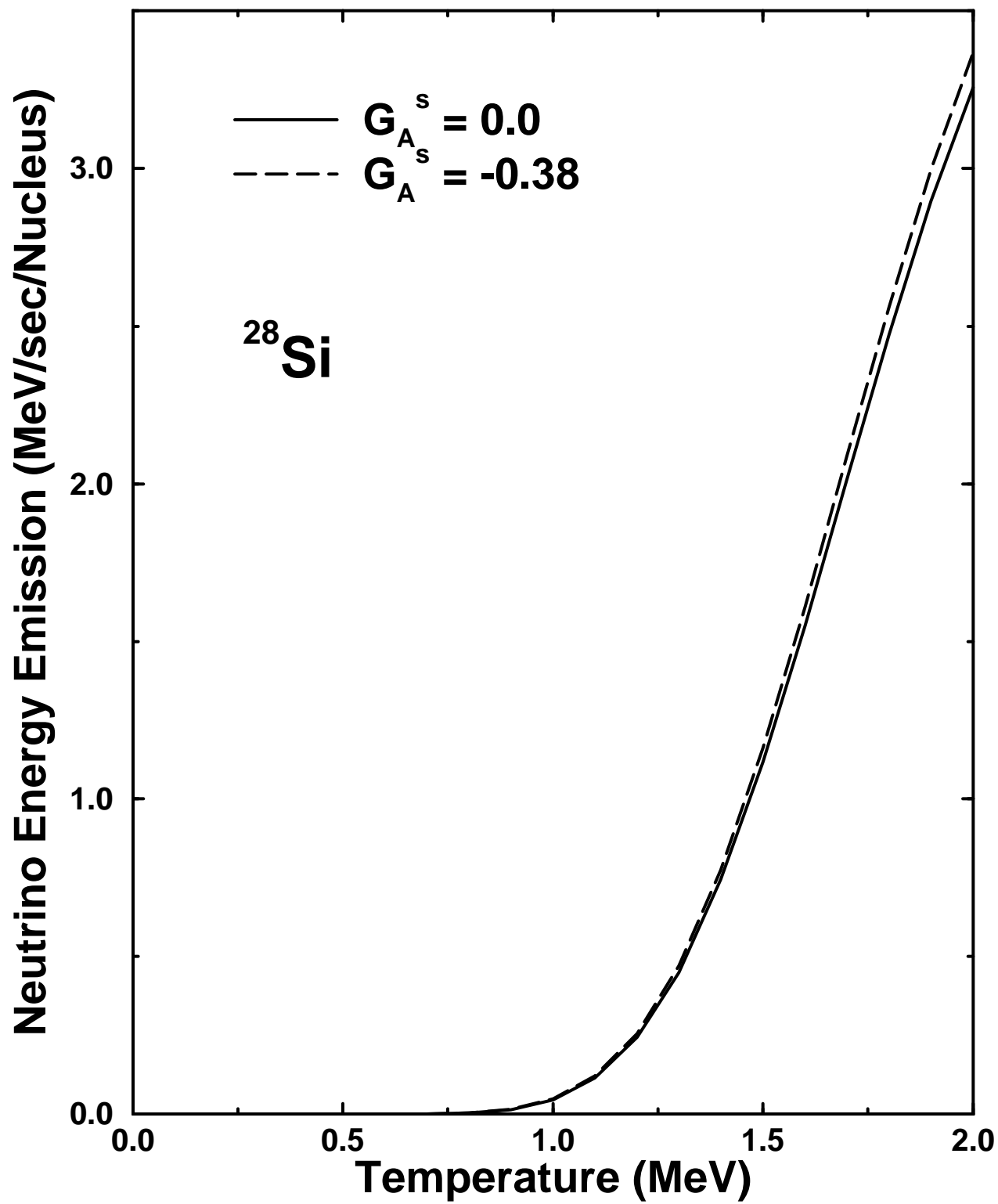


Figure 6

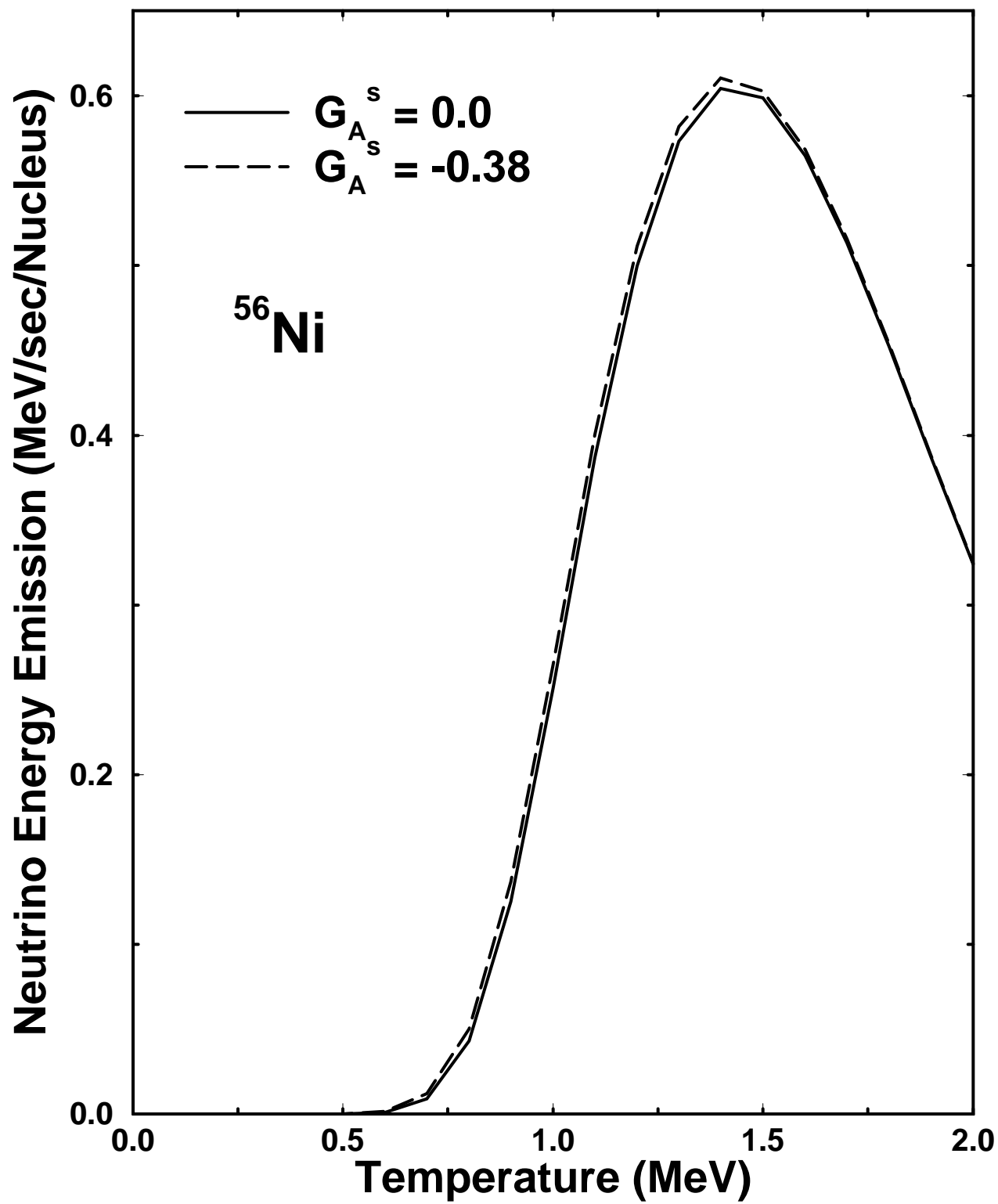


Figure 7

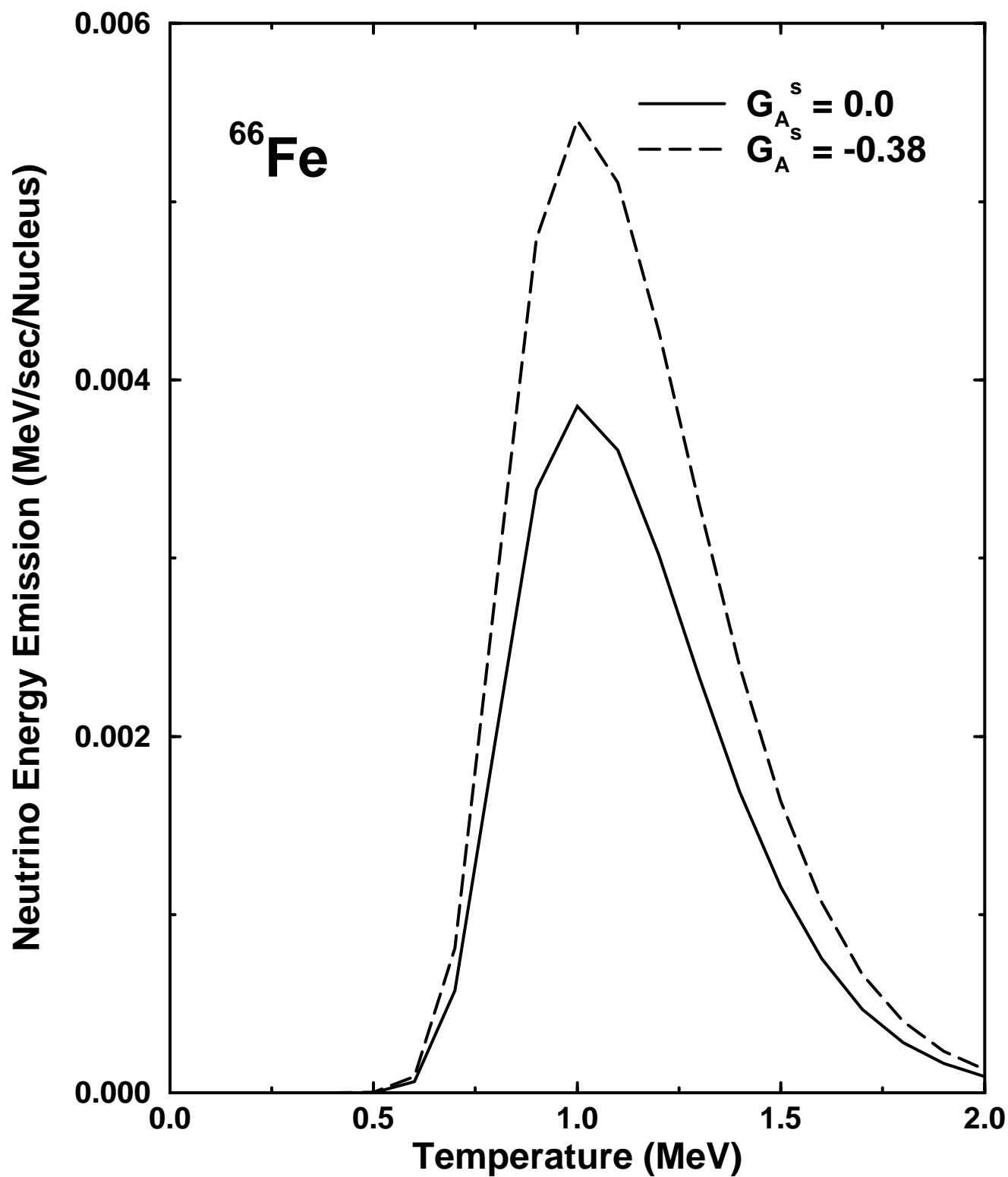


Figure 8